ICAS-80-19.2

A PRACTICAL METHOD FOR PREDICTING FLIGHT-BY-FLIGHT CRACK GROWTH IN FIGHTER TYPE AIRCRAFT FOR DAMAGE TOLERANCE ASSESSMENT

M. Levy*, A. S. Kuo**, K. P. Grube**
Fairchild Republic Co., Farmingdale, N.Y.

Abstract

It has been experimentally observed that the flight-by-flight crack growth rate, "da/dF", under fighter type spectra, can be uniquely related to the stress intensity factor per unit stress, "α", for various forms of 2024-T3 type aluminum alloys. The crack growth analysis method based on this observation is shown to be more effective in terms of accuracy and computer time than the standard cycle-by-cycle integration method. This experimental approach was extended to include spectrum variation, stress level differences, various initial flaw and geometry configuration, and load transfer effects. In selected cases, the technique of developing experimental crack growth curves derived directly from fractographic analysis of specimens tested with periodic marker sequence loadings is discussed. The expansion of the "da/dF" vs. "α" method is shown as a useful and viable tool in performing the fatigue crack growth analyses in support of the A-10A Damage Tolerance Reassessment task.

Nomenclature

A	=	effective crack length
a	=	crack length measured on the surface
$\frac{da}{dF}$	=	crack growth rate for randomized flight-by-flight spectrum
$\frac{da}{dN}$	=	constant amplitude crack growth rate
c	=	crack length measured along edge of a hole
c^o	=	fraction of load transfer
D	=	hole diameter
F	=	1 life of randomized spectrum A-10A
K	=	stress intensity factor
ΔK	=	stress intensity factor range
R	=	stress ratio
s	=	stress level ratio
t	=	thickness
W	=	width
W_p	=	effective width for load transfer
α	=	stress intensity factor per unit stress
σ	=	stress
$\bar{\sigma}$	=	root-mean-square of stresses in spectrum

Superscripts and Subscripts

c	=	critical
eff	=	effective
f	=	final
max	=	maximum
min	=	minimum
o	=	initial

I. Introduction

Since the evolution by the U.S. Air Force of the design philosophy that cracks are assumed to be initially present in all airframe Safety of Flight Structure#, the objective of accurately predicting crack growth in these structures without incurring the penalties of costly and time consuming computer usage has become of particular importance. For typical damage tolerance design[1] and assessment in fighter type aircraft, many fracture critical areas have to be examined. Simplification of the analysis procedures which can readily be verified by coupon testing is a key ingredient to accurately and more economically performing the damage tolerance design and assessment task. In an expansion of the existing fatigue crack growth prediction concepts[2,3,4,5,10] this paper proposes a correlation between the slope of the crack growth vs. flight curve, da/dF, which is reduced from coupon test data, and the stress intensity factor per unit stress, α. This correlation is closely bounded for 2024-T3 type aluminum alloys subject to given random fighter type flight-by-flight stress spectra. The work previously presented in ref (23) formed the basis for the material presented herein. Additional test data now available provides greater support for the correlation and permits the rapid evaluation of spectrum sensitivity over the range of expected flaw size and shape. An experimental relationship was established and used to show how an analytic retardation model might be selected and verified. The important follow-on result, however, is that a single relationship can be used for crack growth predictions in typical aircraft structural geometries subjected to random fighter type similar stress spectra characterized by various related stress levels.

The first part of the paper presents the details on the stress spectra and the coupon tests. In the second part, the development of the crack growth equations, the consolidation of all the experimental data and the description of the data after consolidation by the governing equations

Safety of Flight Structure is defined in MIL-A-83444 as structure whose failure could cause direct loss of an aircraft, or whose failure, if remained undetected, could result in the loss of an aircraft.

* System Design Engineer

** Sr. System Design Engineer

are presented. Lastly, the relationship to the analytic approach of crack growth prediction with retardation and one example of the use of the results for life prediction of a typical structure encountered in fighter aircraft design are given.

II. Spectrum

The flight-by-flight spectrum used for the main part of this study was the 262000 cycles per lifetime A-10A composite maneuver spectrum derived from recent usage of the aircraft. This spectrum is one of the more severe fighter aircraft spectra flown today, as shown in Figure 1. The spectrum considered for the sensitivity portions of the study was the original specification spectrum for the A-10A aircraft used in the full scale development phase of the A-10A design. This spectrum, also shown in Figure 1, consisted of 394000 cycles per lifetime and illustrates the range of potential usage that can occur during the life of a fighter type aircraft. The generation of the flight-by-flight sequence used in test was accomplished by means of a random number generator computer routine operated against the approximately 200 unique maneuver conditions of each subject spectrum in a descending gross weight pattern.

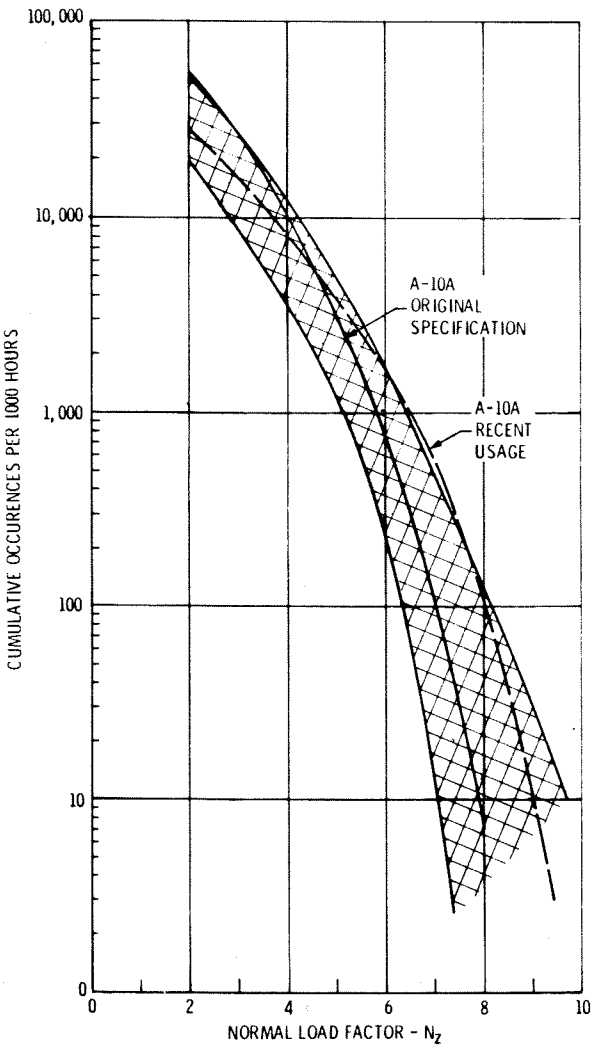

Figure 1. Exceedance Limits for Fighter Aircrafts vs. A-10A

A mission mix of eleven separate missions formed the composite. A representative sequence of ground maneuver conditions is interspersed between flights in the random flight-by-flight sequence used in test. The resulting flight-by-flight random sequence is a repeatable segment equal to 4% of one lifetime. Occurrences of maneuver conditions not repeatable in each 4% random sequence are randomly distributed within each flight to achieve the correct amount of occurrencies per lifetime of these conditions. Approximately 3000 flights make up one lifetime or 6000 flight hours. Stress spectra representative of the inboard lower wing cover of the A-10A aircraft were calculated for each unique spectrum condition using reference stress levels of 39.28 and 35.2 ksi as the maximum spectrum stresses.

III. Tests

Test specimens were manufactured from shot-peened 2024-T3511 extrusion material which was nominally 0.250 inch thick. Several specimen configurations were tested. These consisted of low (≈5%), high (≈15%) load transfer and no load transfer (filled or open hole) specimens. Load transfer specimens were manufactured within hole tolerance specifications which permit a range of pin fit from slight clearance (.0015 inch on the diameter) to slight interference (.0035 inch on the diameter). Typical specimen geometry is shown in Figure 2.

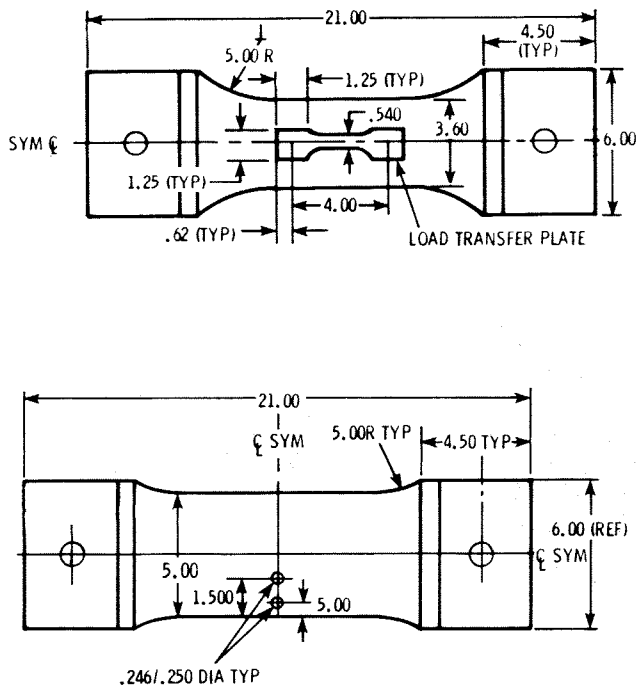

Figure 2. Typical Test Specimens

Each specimen was precracked initially to ideally produce a quarter circular corner flaw at the edge of a hole in the test section. Precracking consisted of the introduction of a 45° notch through electrical discharge (elox) in an initial hole smaller than the final required size hole. Cycling at constant amplitude made this flaw grow into a sharpened fatigue crack of the size desired after the initial hole was reamed to final size. In many cases

however, the actual resulting flaw tended to be elliptic in cross-sectional shape. For those cases, the actual initial flaw size and shape was accounted for using the appropriate stress intensity solution given in the Appendix. The observed crack growth behavior is presented as surface crack length versus fraction of life expended. Determination of corner crack shape during the interim period prior to breakthrough was obtained from fractographic examination of the specimen fracture surface.

For a majority of the test specimens, crack length measurements were made visually using a 30X microscope. For the remaining specimens, visual measurements were augmented with growth markings observed from fractographic analysis of the specimen fracture faces. These markings resulted from an applied ordered loading sequence interspersed at regular intervals in the random flight-by-flight test loading. Research into the type of ordered loading sequence required, indicates that for 2024-T3 type material subjected to random flight-by-flight loading at maximum gross stresses near the material yield point, a low-high cyclic arrangement will successfully mark the fracture face with a distinguishable tell-tale pattern (Ref. 16). For a typical test specimen in this group, Figure 3 shows the marking growth pattern. In these tests, the marker sequence consisted of four repeatable one percent segments of the random flight-by-flight cyclic loading arranged in a low to high stress pattern. Each one percent sequence contained exactly the same number of cyclic occurrences that the random flight-by-flight segment contained, thus preserving the total number of cycles. The marking sequence was applied at approximately each 25% of life during testing. Fractographic analysis of specimens and crack growth analysis of these specimens (Ref. 16) indicated that no anomalous crack growth behavior was exhibited by the application of the marker sequence. Crack growth curves were then obtained directly by matching up marker indications with test time application while comparing measured lengths.

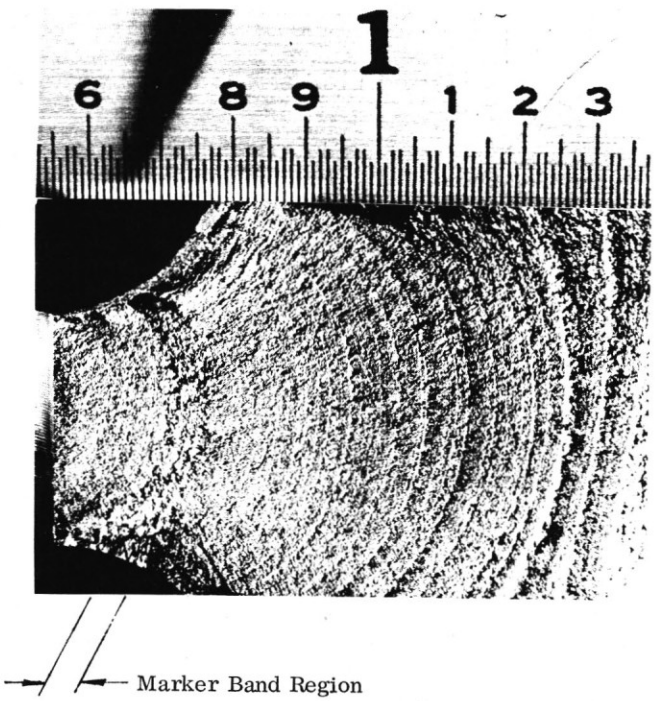

Figure 3. Fracture Surface with Marker Band

Tests were conducted in hydraulic load frames operated through a closed loop computer-directed control and supervising system. The applied loads were maintained within a ±1% of the required values.

IV. A Crack Growth Prediciton Method

The progress of fatigue and fracture research has made it possible to predict fatigue crack growth more accurately than ever before. A great advance is the utilization of the stress intensity factor K, to characterize fatigue crack growth shown by Paris[2]. Fatigue crack growth rate can be uniquely related to K, because K is able to represent the combined effect of geometry and load on the crack tip deformation. Therefore, coupon testing data can be used directly to predict crack growth in actual structures using a cycle-by-cycle integration method. This approach has been shown to be very successful for simple cases of constant amplitude fatigue loading.

In actual aircraft service conditions, loads are far from being constant. Hence, variable amplitude flight-by-flight randomized spectra are now typically used to simulate actual service loads. In the prediction of crack growth under variable amplitude load spectra, the results are often found to be too conservative if load-interaction is not properly treated. Willenborg[7], Wheeler[8] and closure models[9] are the popular approaches to treat the crack growth retardation behavior due to over-load effect. These models have shown various degrees of success. However, in order to have full confidence in predictions using these techniques experimental verification and/or adjustment is required.

The cycle-by-cycle integration method is the basic way of predicting crack growth under any kind of load spectrum. If analyses are needed for several fracture critical locations subjected to the same or similar load spectrum, the cycle-by-cycle integration method becomes costly. A recent suggestion for crack growth prediction for aircraft is to use da/dF (crack growth per flight) instead of da/dN (crack growth per cycle)[10,13,15]. In the da/dF approach, the cycle-by-cycle integration method is, again, needed to obtain da/dF for a specific stress spectrum. The resulting da/dF can then be used to predict crack growth of other locations subjected to the same stress spectrum without resorting to the integration of crack growth through all of the load-cycles in the given spectrum. Substantial computer CPU time, however, can be saved with the da/dF approach when da/dF is developed directly from experimental crack growth test data. In addition, this will provide an avenue to assess various spectra of related stress levels as will be shown.

Paris[2] suggested that da/dN of variable amplitude random load spectra can be characterized by:

$\bar{K}_{max} = \bar{\sigma}_{max}\alpha$ where $\bar{\sigma}_{max}$ is the root-mean-square

of stress cycles in a spectrum and α ($=K/\sigma = \sqrt{\pi\, a}\,\gamma$) is the stress intensity factor per unit stress (or stress intensity factor coefficient). The theoretical and analystical works of Smith[3], Swanson et al[4] and Barsom[5] support Paris' suggestion. Paris' approach was applied to da/dF by Gallagher[13] who, in the light of the works of Paris[2] and Forman et al[11] proposed the following equation form for correlation of da/dF vs. $\bar{K}_{max}$ data,

$$\frac{da}{dF} = \frac{C\bar{K}_{max}^{m}}{K_c - \bar{K}_{max}} \qquad (1)$$

where K_c is fracture toughness; C and m are empirical constants to be determined from a best data fitting process. Schijve[12] also pointed out that da/dF vs. K_{max} approach could be applicable to similar spectra. According to Equation (1), experimental data points of da/dF vs. K_{max} for similar spectra should fall into a line. Gallagher and Stalnaker's[13] test data for bomber type spectra with three different stress levels indicate good correlation between da/dF and K_{max}. The bomber type spectrum, however, is a relatively mild spectrum in comparison with typical fighter spectra. In a bomber type spectrum the load interaction is considerably less severe than in the fighter spectrum, making the burden of proof for da/dF vs. K_{max} for fighter spectra fall on new test substantiation.

Since the characteristic stress intensity factor K_{max} is defined as $K_{max} = \sigma_{max}\sqrt{\alpha}$ as mentioned in the last paragraph, a natural alternative to da/dF vs. K_{max} is da/dF vs. α. Brussat[14] has used $\alpha = K/\sigma$ to characterize variable amplitude crack growth. The use of α would circumvent the need to justify σ_{max} as a characteristic stress for a spectrum. As a matter of fact σ_{max} is a constant for a specific spectrum and hence there is no need to consider it at all. For similar spectra, two approaches are proposed in this paper to account for the differences in stress levels among each individual similar spectrum. The stress level ratio, s, which is defined as the ratio of the maximum peak stress in a less severe stress spectrum to the maximum peak stress in the most severe or baseline reference stress spectrum, is an index to represent the severities among similar spectra. The word "similar" in this context means that there exists, roughly, a one-to-one correspondence in each stress cycle for each similar spectrum and the magnitude of each stress cycle in a spectrum can be scaled from that of the reference spectrum, which is usually chosen to be the severest spectrum.

One approach to account for stress level of a spectrum is to use effective stress intensity factor coefficient, $\bar{\alpha} = s\alpha$. The da/dF is then characterized in terms of $\bar{\alpha}$ instead of α. A plot of experimental da/dF vs. $\bar{\alpha}$ data points from spectra with different stress levels should fall into a narrow band. The following form of equation is proposed for da/dF vs. $\bar{\alpha}$ correlation,

$$\frac{da}{dF} = \frac{C\bar{\alpha}^m}{\alpha_c - \bar{\alpha}} \tag{2}$$

where α_c, C and m are empirical constants to be determined from a best data fitting procedure. It should be noted that α_c for a group of similar spectra is not a purely empirical constant although it is determined from a data fitting procedure. The magnitude of α_c depends, to a great extent, on the fracture toughness of the material under investigation. The meaning of α_c is in parallel to that of K_c.

The other approach to account for stress level of a spectrum is proposed in the following equation,

$$\frac{da}{dF} = \frac{C\alpha^m}{\frac{\alpha_c}{s} - \alpha}\, s^n \tag{3}$$

If n is equal to m-1, Equation (3) is identical to Equation (2). α_c, C, m and n are empirical constants to be determined by best data fitting procedures. The implication of Equation (3) is that if $(da/dF)/s^n$ is plotted against α for spectra with different s then the test data shall fall into a narrow band. Although the implementation of Equation (3) would require more effort, it does offer more freedom via the constant "n" to find an equation which best fits test data.

The two approaches described in the last two paragraphs for the characterization of experimental da/dF shall be verified in the coming sections of this paper. While they appear slightly different in form, both Equations (2) and (3) are, in essence, based on the same concept that da/dF can be uniquely related to α.

With the empirical da/dF vs. α relation available, the crack growth integration method briefly outlined below can be used to obtain Damage Tolerance Life interval, ΔF_i, for extending a crack from a_{i-1} to a_i.

$$\frac{da}{dF} = f(\alpha) \tag{4}$$

then;

$$dF = \frac{da}{f(\alpha)} \tag{5}$$

$$\Delta_{F_i} = \int_{a_i - 1}^{a_i} \frac{da}{f(\alpha)}, \quad i = 1, 2, \ldots N$$

Since α can hardly be expressed in explicit form as a function of "a" for actual aircraft structures, Equation (5) can not be integrated to obtain closed form solutions. Numerical integration methods, e.g. Trapezoidal or Simpson's rule, are usually used to evaluate Equation (5). The accumulated Damage Tolerance Life, F_i, required to extend crack from a_o to a_i is:

$$F_i = \sum_{j=1}^{i} \Delta F_j \tag{6}$$

The thus calculated paris of points, i.e. a_i vs. F_i, are used to construct the fatigue crack growth vs. life curve. It is obvious that the numerical integration of Equation (5) would need much less CPU time than the cycle-by-cycle integration method.

The proposed experimental da/dF vs. α correlation is a reliable and economical approach to predict fatigue crack growth under similar spectra, which will ensure the safety and durability of fleet aircraft. It is recognized that load-interaction often handicaps an accurate theoretical prediction of crack growth under variable amplitude stress spectrum. Broek and Smith[15] reported that a wide range of life to reach the same crack length was obtained using different load-interaction models such as Willenborg, Wheeler and closure models. In order to make reliable predictions, any load-interaction model would need adjustments according to experimental data. In this way, the sum of the costs due to analytical and experimental works will be enormous. A practical approach would be using the experimentally determined da/dF vs. α data as the base of analysis. The use of experimental da/dF would avoid the analytical difficulties with load-interaction. The use of da/dF instead of cycle-by-cycle integration would substantially simplify analysis and reduce (CPU) time in analyzing a group of fracture critical locations subjected to similar spectra. Test data of da/dF for three stress levels would likely be sufficient to establish a generalized da/dF vs. α data base such as Equations (2) and (3) for structures subjected to similar spectra.

V. Experimental Results and Discussions

The raw test data are plotted in Figure 4 as curves of surface crack length vs. fraction of crack growth life. Actual test points were replaced with the best fitting smooth curve. Table 1 shows the flaw sizes, and their corresponding growth at successive stages of testing for each individual specimen. The curves in Figure 4 are plotted from the actual initial flaw size of the test specimens to permit a wide range of α to be considered.

In addition to consideration of the initial flaw size, the changing shape of the flaw as it grows into a through the thickness crack is also important.

Figure 5 is a 5X photograph of the fracture surface of a typical test specimen. The photograph indicates that the flaw shape is elliptical before breakthrough and is becoming quarter circular during the transition to breakthrough. Table 1 shows typically that the major part of fatigue life was spent in the period from initial flaw to breakthrough.

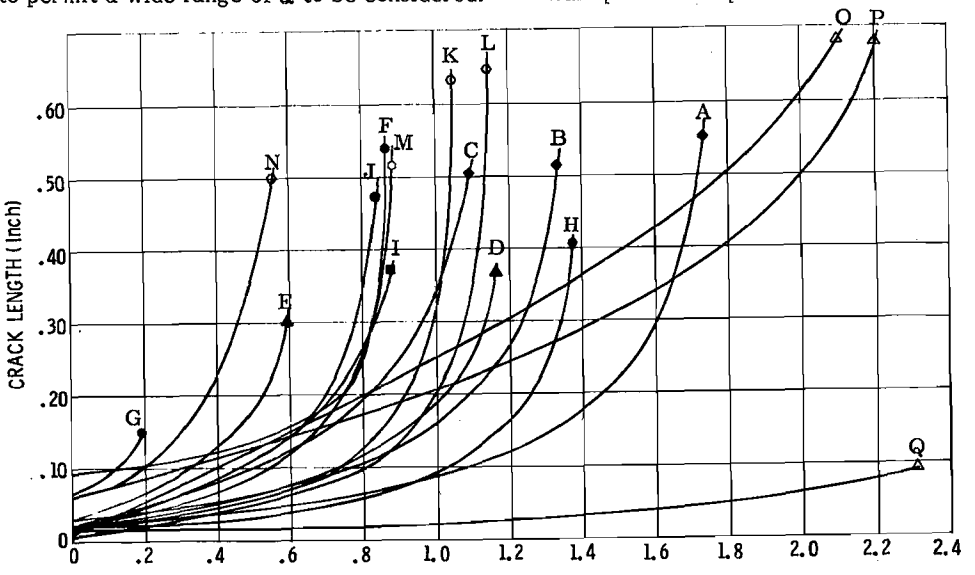

Figure 4. Crack Growth vs. Life Curves

Table 1. Life vs. Crack Length Measurements

- Tests No. A thru N, Usage Spectrum Testing
  Tests No. O thru Q, Original Specification Testing
- Tests No. I, K thru P ~ Open Hole Specimens
- Test No. 9, No Failure Occurred
  Test Stop at 13920 Hours

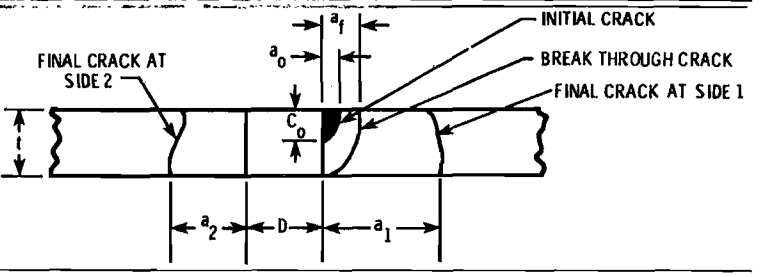

Test No.	Loading Condition		D	Life At Breakthrough	Life At 2nd Crack Initiation	Life At Failure	Initial Crack		Breakthrough	Final Crack		Aspect Ratio	
	Max. Stress (ksi)	Load Trans. (%)	(In)	(Hours)	(Hours)	(Hours)	a_o (In)	c_o (In)	a_f (In)	a_1 (In)	a_2 (In)	a_o/c_o	a_f/t
A	39.28	5.0	0.250	7920	9360	10102	0.018	0.086	0.136	0.390	0.170	0.21	0.62
B	39.28	5.0	0.250	5520	7440	7718	0.027	0.089	0.184	0.440	0.160	0.30	0.84
C	39.28	5.0	0.250	0	6240	6888	0.056	Thru	0.056	0.625	0.250	Thru	Thru
D	39.28	15.0	0.250	3840	5040	6787	0.020	0.079	0.083	0.350	0.290	0.25	0.33
E	39.28	15.0	0.250	1680	1680	3126	0.031	0.080	0.109	0.250	0.240	0.39	0.44
F	39.28	0.0	0.250	4560	1500	5220	0.092	0.189	0.209	0.555	0.105	0.49	0.70
G	39.28	0.0	0.250	720	2 cracks	1200	0.065	0.065	0.095	0.160	0.150	1.00	0.38
H	39.28	0.0	0.375	5520	11040	8280	0.040	0.050	0.075	0.900	0.680	0.80	0.34
I	39.28	0.0	0.250	4080	3360	5078	0.010	0.010	0.362	0.740	0.405	1.00	1.65
J	39.28	0.0	0.040	0	2 cracks	5040	0.030	Thru	0.030	0.600	0.600	Thru	Thru
K	35.10	0.0	0.375	5520	5760	6276	0.025	0.020	0.150	0.700	0.680	0.75	0.68
L	35.10	0.0	0.375	6240	5760	6888	0.005	0.005	0.160	0.840	0.730	1.00	0.73
M	35.10	0.0	0.500	3180	No 2nd	5322	0.020	0.125	0.095	0.542	None	0.16	0.32
N	35.10	0.0	0.500	1800	No 2nd	3384	0.060	0.180	0.143	0.514	None	0.33	0.47
O	35.10	0.0	0.546	1920	No 2nd	13080	0.010	0.010	0.105	0.880	None	1.00	0.35
P	35.10	0.0	0.500	0	No 2nd	13428	0.060	Thru	Thru	0.730	None	Thru	None
Q	35.10	5.0	0.250	None	No 2nd	13920	0.020	0.156	None	0.088	0.200	0.13	0.35

Therefore, it is important to account for flaw shape in calculating stress intensity factor; it is in contrast to the conventional practice of treating a corner flaw as quarter circular. This point is particularly important to the relatively thick sections found in airframe structures. The actual shape of the initial flaw and its changing shape has been accounted for in the analysis of the test data shown in Table 1.

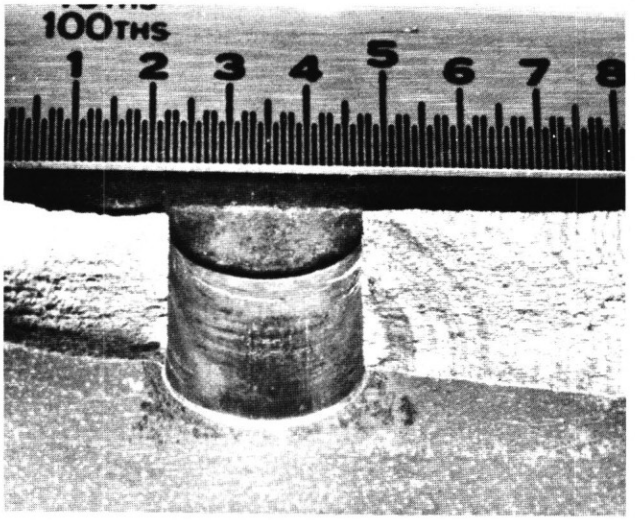

Figure 5. Fracture Surface of a Typical Test Specimen

As a point of reference, Figure 4 shows that high pin load transfer results in a much shorter life than low pin load transfer and that filled hole specimens reach much higher life than open hole specimens.

The test data shown in Figure 4 was evaluated using the seven points incremental polynomial method to obtain da/dF vs. "a" data, where "a" is surface crack length and F is fraction of fatigue life. This method is recommended by ASTM Standards[17] to process da/dN data. The stress intensity factor per unit stress, α for a given flaw configuration was calculated with the method described in the Appendix. The resulting da/dF vs. "a" data and α vs. "a" data were then used to establish da/dF vs. α data for each specimen. Next, the da/dF vs. α data were characterized in terms of the two proposed methods mentioned in the last section to account for the spectrum stress levels.

Figure 6 shows a composite of all the high stress level data points plotted as da/dF vs. α (s=1). The method of least squares was used to evaluate the unknown constants of Equation (2) and is shown as Equation (7).

$$\frac{da}{dF} = \frac{0.681\,(s\alpha)^{2.77}}{1.5 - s\alpha} \quad (s = 1) \qquad (7)$$

The coefficient of correlation and modified standard error are 0.9944 and .2500 respectively.

Figure 6 also shows a solid line representing Equation (7) and two dashed lines representing one standard deviation from Equation (7). Figure 6 shows all data points fall into a narrow band characterized by plus and minus one standard deviation regardless of geometric factors. This relationship appears to corroborate the scatter exhibited by raw da/dN data for 2024 aluminum alloy.

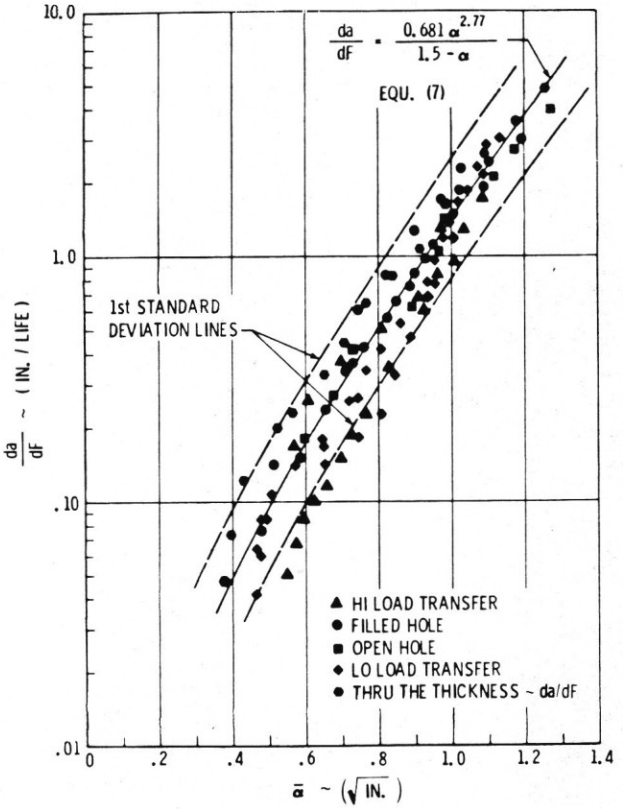

Figure 6. da/dF vs. for High Stress Level

Figure 7 shows a composite of the intermediate stress level data points plotted as da/dF vs. α (s=0.893). Equations (2) and (3) with coefficients evaluated are shown in this plot as the solid line. Equation (7) for s=0.893 becomes:

$$\frac{da}{dF} = \frac{0.498\,\alpha^{2.77}}{1.5 - 0.893\alpha} \qquad (7a)$$

This approach to evaluate other stress level ratios of the same spectrum is the alternate to the use of Equation (3). Equation (3) was evaluated by retaining the same constant C and the exponent m evaluated against α only in Equation (7). The exponent n was determined by testing for minimum standard error and minimum deviation from unity in correlation. Equation (3) with all constants evaluated is shown in Equation (8) and Figure 7.

$$\frac{da}{dF} = \frac{0.681\,\alpha^{2.77}\,s^{4.0}}{\frac{1.5}{s} - \alpha} \qquad (8)$$

A comparison of Equation (7) with Equation (8) indicates that the value for the constant n to best fit the intermediate stress data points is 4.0 instead of 1.77 (n=m-1=2.77-1=1.77) as derived from Equation (7). This difference in exponents is a measure of the true sensitivity of stress level change as it affects results obtained in actual testing. The coefficient of correlation and modified standard error for Equations (7a) and (8) which characterize the intermediate stress level are 0.363, 1.357 and 0.076, 0.952 respectively.

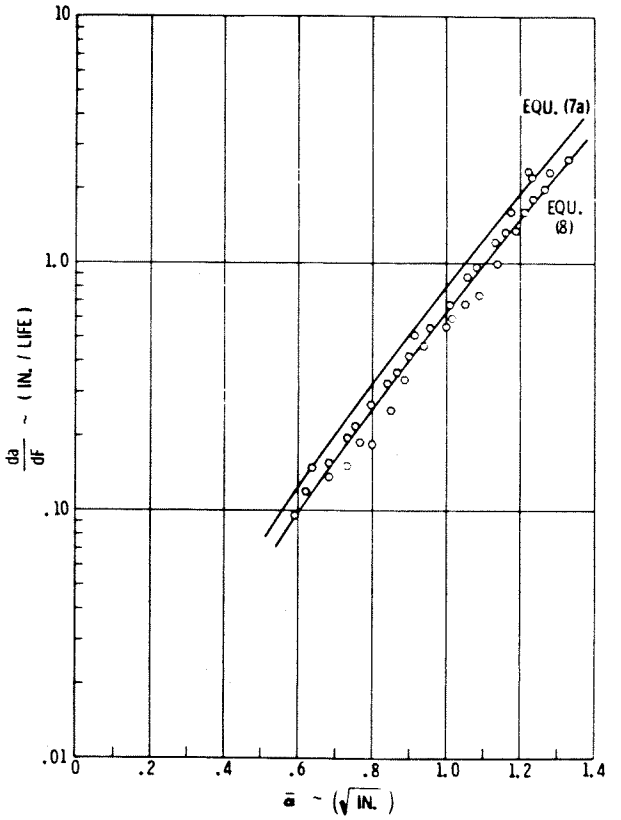

Figure 7. da/dF vs. α for Intermediate Stress Level

The aforementioned coefficients of correlation and modified standard errors are statistical quantities to measure the degree of correlation and fit between test data and Equations (7a) and (8) respectively. The slight differences among these numbers indicate that either Equation (7a) or Equation (8) can be closely fit to test data. However, Equation (8) as seen in Figure 7 provides a somewhat better fit and offers greater flexibility in accounting for inherent material/test variables. Equation (8) reduces to Equation (7) with s=1 (high stress level) and as indicated possesses the built-in precision via the constant n to characterize similar spectra of different stress level ratios. The direct implication is that for the same α , $(da/dF)/s^n$ obtained from spectra of different stress level ratios would be the same.

It should be emphasized that the experimental da/dF data of this investigation were collected under a variety of initial flaw configurations, loading conditions and specimen geometries. Therefore, Figures 6 and 7 together with Equations (7) and (8) sufficiently demonstrate that experimental da/dF can be uniquely characterized with the stress intensity factor per unit stress, α . Equations (7) and (8) will be the bases for crack growth analysis in an example to be described later.

Figures 6 and 7 can serve as baseline data for verifying and/or adjusting any theoretical load-interaction models. Since the crack length at various stages of life is obtained by an integration of $da/dF=f(\alpha)$ relation, any theoretical prediction method should yield a "$f(\alpha)$" which falls onto a band defined by tested da/dF vs. α data. Any deviation from test data would necessitate adjustments of the candidate theoretical load-interaction model. It has been reported that different Wheeler constants were needed for a reasonable fit between test and theoretical crack growth vs. life curve even though specimens of different geometry were made of the same material and were tested under similar or same load spectra[15,19]. A common practice of dealing with this problem is to use an average Wheeler constant as a compromise among specimens. An alternative is suggested in Figures 6 and 7, that the appropriate Wheeler constant should be selected such that the resulting da/dF would fall onto tested da/dF. In this manner, one could have a direct quantitative feeling of the compromise among specimens for the Wheeler constant selected.

Two theoretical curves predicted by the cycle-by-cycle integration method using the Willenborg and Wheeler models are shown in Figure 8. Both the Willenborg and Wheeler models fall reasonably well within the test data. The Wheeler constant selected for this comparison was 3.0. The driving factor behind the placement of these theoretical curves is the choice of the material da/dN properties. The Willenborg model can hardly be adjusted to conform with test data except through the change of these baseline da/dN material properties which must be statistically demonstrated. Often, these properties are selected from published data independently of test specimen results which are used primarily to determine crack growth behavior under spectrum loading directly.

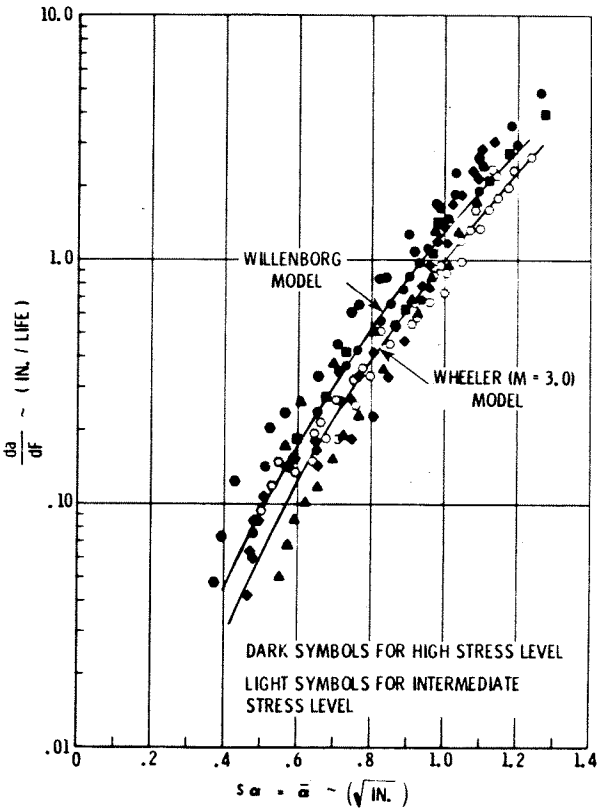

Figure 8. Cycle-by-Cycle Integration Method vs. Test Data

In trying different Wheeler constants for best fit to test data, it was observed that the predicted curves corresponding to different Wheeler constants are approximately parallel to one another. Consequently, if this group of curves are not parallel to the band defined by test data, no single Wheeler constant can be selected such that the predicted Wheeler curve will follow the shape of test band for the whole range of α under investigation. By experience the general formulation of the Wheeler

equation does not allow for shape variation with respect to the individual crack growth range with respect to test data although the end failure point can be approached. This supports the notion of multiple constants over the range of growth as suggested above. The agreement between predicted and test crack growth vs. life curve is often the result of a fortuitous balance between the over-estimation and under-estimation of da/dF in the low and high α regions respectively. In general the validation of analytic load interaction retardation models by the da/dF method is a complicated process often involving the use of trial and error. It can also be seen that in the case of the Wheeler model, the actual constant can become a variable over the range of α.

VI. Spectrum Correlation

The evaluation of the effect of spectrum variations on life is addressed in this section. In Section 2, the original A-10A specification spectrum was introduced and was compared to the A-10A recent usage spectrum (Figure 1). It is not uncommon in the course of the life of an aircraft system for usage to change. In addition, the usage may change during the performance of full scale and/or major component testing. For this reason it is of paramount importance to assess the sensitivity of one spectrum against the other and to determine equivalency of test time (degree of over or under test) for those tests in progress at the time a spectrum change is recognized.

The "da/dF" vs. "α" approach was successfully employed in the A-10A spectrum evaluation. Of major importance is the fact that the A-10A original specification spectrum could be characterized by "da/dF". This in itself lends additional credibility to concluding that the "da/dF" vs. "α" approach can be successfully used for all fighter type spectra. Figure 9 shows the composite of data points plotted for the intermediate stress level (s=0.893) for the subject spectra (Ref. Table 1). Also shown are the best fit da/dF vs. α equations for these data points. For the recent usage spectrum, this is Equation (8) and for the original specification spectrum, the best fit equation obtained from the method of least squares is shown as Equation (9):

$$\frac{da}{dF} = \frac{.1106\,\alpha^{4.742}}{1.68 - \alpha} \qquad (9)$$

Modified standard error = .078
Coefficient of correlation = .985

Spectrum changes can now be evaluated using Equation (8) and (9) directly, realizing that the sensitivity is also affected by the limits of initial and final crack sizes and the amount of test time at spectrum transition with the same stress level ratio. Substitution of Equations (8) and (9) into Equations (5) and (6) for each spectrum to calculate values of F_i and a_i allows ratios of life vs. crack size to be computed. These values are compared for degree of spectrum sensitivity over accumulated time since, as can be seen in Figure 9, the sensitivity is not expected to be a constant value.

From review of Equation (7a) and (8), it is reasonable to conclude that stress level ratio plays a role in the spectrum sensitivity. It is expected that the effect two spectra have on life at different stress level ratios would be different.

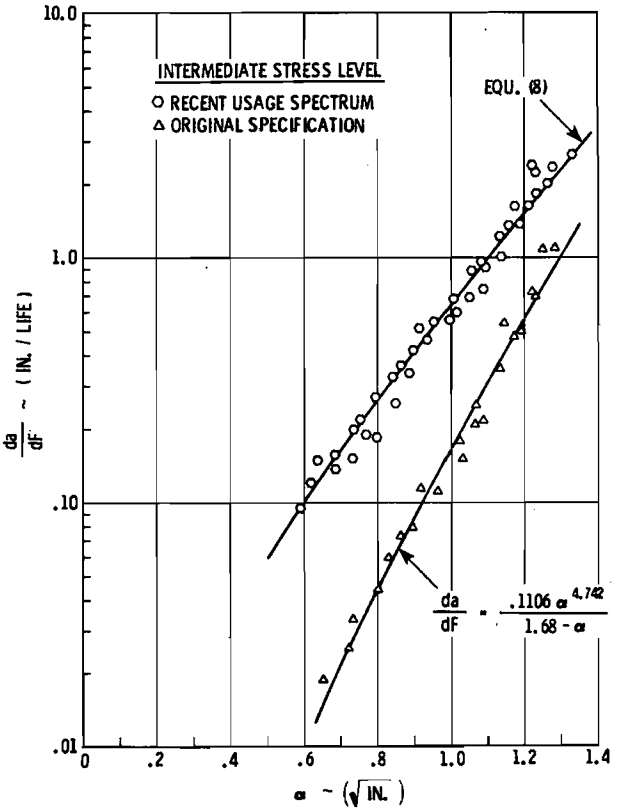

Figure 9. Spectra Correlation for Intermediate Stress Level

VII. Example

An illustration of how the da/dF vs. α concept is used in predicting life for damage tolerance assessment is described. The structure selected for this example is a spar cap element located in one of the fracture critical areas on the lower wing panel of the A-10A aircraft. The spar cap structure in general is represented by the test specimens outlined in Table 1. The cap structure operates at a stress level ratio equal to 0.924 and is subject to high load transfer. Fasteners joining the cap to adjacent skin structure are transition fit. The cap is analyzed for damage tolerance as an independent element for qualification by slow crack growth. The initial flaw was selected as a 0.005 inch quarter circular crack on the edge side of the hole to allow for a greater range of comparison between the various crack growth prediction methods. The analytic prediction by da/dF was performed using Equation (8) integrated by Simpson's Rule,

$$\frac{da}{dF} = \frac{0.681\,\alpha^{2.77}\,s^4}{\frac{1.5}{s} - \alpha} \qquad s = 0.924$$

$$\frac{da}{dF} = \frac{0.571\,\bar{\alpha}^{2.77}}{1.5 - \bar{\alpha}} \qquad \bar{\alpha} = 0.924\alpha \qquad (10)$$

$$F_i = \int_{a_i - 1}^{a_i} \frac{1.5 - \bar{\alpha}}{0.571\,\bar{\alpha}^{2.77}}\,da, \quad i = 1, 2, \ldots N$$

The relationship between "a" and "α" was generated according to the Appendix for use in the integration of Equation (10).

The Willenborg and Wheeler models were applied using the cycle-by-cycle integration method and da/dN data in the form of Forman's equation;

$$\frac{da}{dN} = \frac{1.799 \times 10^{-7} \ \Delta K^{3.201}}{(1 - R)\ 83 - \Delta K} \qquad (11)$$

The constants in Equation (11) were obtained from the best fit of da/dN data for 2024-T3 plate material[18]. As indicated in Figure 10, the Willenborg model is quite conservative, while the Wheeler model appears to predict well. However, the accuracy of the analytic analysis methods is highly dependent on material da/dN choice. In contrast, the da/dF method is tied directly to material crack growth behavior of the material and geometry representative of the real structure.

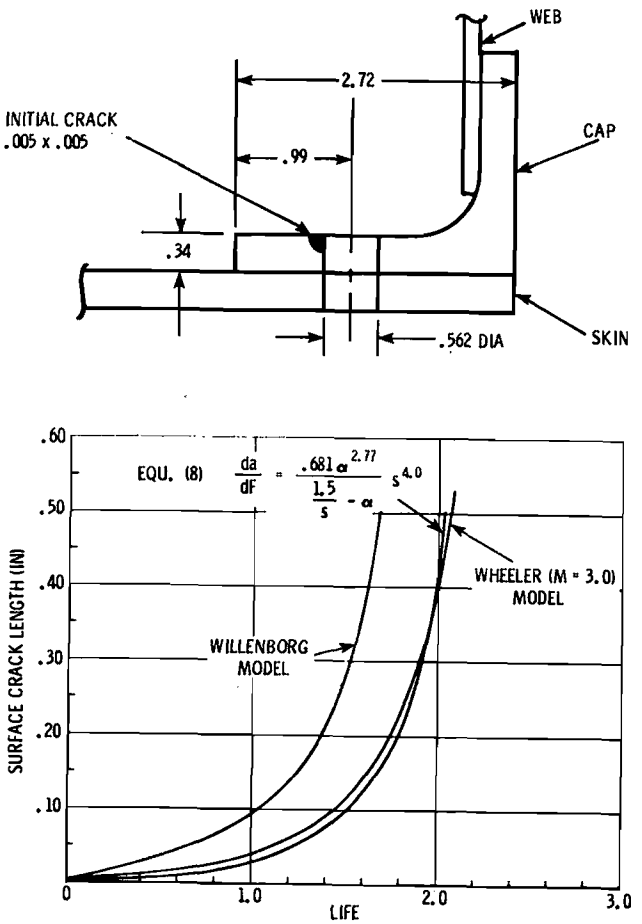

Figure 10. Crack Growth Prediction

The point that must be emphasized is the accuracy of predicting life and the cost in terms of computer CPU time generating crack growth data which is approximately 15:1 in favor of da/dF vs. α type integration.

VIII. Conclusions

The following conclusions are offered based on the analysis of the test results presented herein:

(1) da/dF vs. α data collected from tests under various specimen geometry and similar fighter type stress spectra fall into a narrow band. This fact suggests that da/dF can be characterized by a single parameter α.

(2) The differences in stress level among similar spectra can be solved by either replacing α with $s\alpha$ or modifying da/dF with a factor $1/s^n$.

(3) The application of experimental da/dF vs. α relationship for analyzing crack growth life is a reliable and economic way to fulfill the aircraft damage tolerance design and assessment task.

(4) The experimental da/dF vs. α relationship can be used to verify and adjust analytical load-interaction models.

(5) The experimental da/dF vs. α relationship can be used to evaluate the sensitivity of a structure to different (non-similar) spectra.

Appendix

The Stress Intensity Factor (SIF) for an elliptical corner flaw at the edge of a hole is known to vary along the crack front. The majority of specimen tests used in development of this paper show change in the aspect ratio of the crack. To account for this change, actual initial and breakthrough crack aspect ratio are considered. The crack shape between the two intervals is assumed to change proportionally. The expression for SIF used in this analysis accounts for the change in shape. Basically, it has the form of an embedded elliptical flaw with the appropriate geometric and loading corrections. Hence $\alpha = K/\sigma$ will have the following expression:

$$\alpha = \sqrt{\pi a}\ (\lambda)\ (\beta)\ (f_B)\ (\gamma) \qquad (1A)$$

where:

$$\lambda = \frac{1.12}{\Phi}\ (\sin^2\varphi + (\tfrac{a}{c})\cos^2\varphi)^{1/4} \text{(Open Hole)}$$

$$\lambda = \frac{1}{\Phi}\ (\sin^2\varphi + (\tfrac{a}{c})^2\cos^2\varphi)^{1/4} \text{(Filled Hole)} \qquad (2A)$$

The expression in the parentheses is evaluated at two locations along the crack front. A weight average is then used to approximate a single value of SIF which is assumed representative for the crack front.

Φ is an elliptical integral of the second kind and it is well defined in the literature to be:

$$\Phi = \int_0^{\pi/2} (1 - \frac{c^2 - a^2}{c^2}\sin^2\varphi)^{1/2}\, d\varphi \qquad (3A)$$

"β" is the finite width correction for symmetrical and unsymmetrical crack[21].

f_B is the Bowie solutions for one or two unsymmetrical cracks[20].

"γ" is the load transfer correction obtained from superposition of the tension load and pin load solutions:

$$\gamma = (1 - 0.5c^{\circ}) + \frac{c^{\circ} W_p}{2\pi A}\sqrt{\frac{2A}{\frac{D}{2} + a} - 1} \qquad (4A)$$

where:

$A = (D + a)/2$ for 1 crack

$A = \frac{D}{2} + a$ for 2 cracks

To account for the transition from a corner crack to through the thickness crack a modification of the empirical formula suggested by Ref. 22 was used,

$$\alpha^{\text{corner}}_{\text{final}} = \frac{\alpha \text{ corner} + 2\left(\frac{c}{t}\right)^2 \alpha \text{ thru}}{2\left(\frac{c}{t}\right) + 1}, \quad t \geq C \geq \frac{t}{2} \qquad (5A)$$

$$\alpha^{\text{corner}}_{\text{final}} = \alpha \text{ corner (eq. 1A)}, \quad 0 < C < \frac{t}{2}$$

where:

$$\alpha_{\text{thru}} = \sqrt{\pi a}\,(f_B)\,(\beta)\,(\gamma) \qquad (6A)$$

IX. References

1. USAF Military Specification - MIL-A-83444, 1974.
2. Paris, P.C., "The Fracture Mechanics Approach to Fatigue", Fatigue - An Interdisciplinary Approach, Proc. of the 10th Sagamore Army Materials Res. Conf., ed. by J.J. Burke, N.L. Reed and V. Weiss, Syracuse Univ. Press, 1964, pp 107-132.
3. Smith, S.H., "Fatigue Crack Growth under Axial Narrow and Broad Band Random Loading", in Acoustic Fatigue in Aerospace Structures, ed. by W.J. Trapp and D.M. Forney, Jr., Syracuse Univ. Press, 1965, pp 331-360.
4. Swanson, S.R., Cicci, F., and Hoppe, W., "Crack Propagation in Clad 7079-T6 Aluminum Alloy Sheet Under Constant and Random Amplitude Fatigue Loading", in Fatigue Crack Propagation, ASTM STP 415, 1967, pp 312-362.
5. Barsom, J.M., "Fatigue - Crack Growth Under Variable Amplitude Loading in ASTM A514B Steel", in Progress in Flaw Growth and Fracture Toughness Testing, ASTM STP 536, pp 147-167.
6. "Development of Flight-by-Flight Spectra for A-10A PDV Tests", Rev. C, Fairchild Republic Co., Report No. FRC SA160R9403, 14 May 1979.
7. "Willenborg, J., Engle, R.M., and Wood, H.A., "A Crack Growth Retardation Model Using an Effective Stress Concept", AFFDL, Report No. TM-71-1-FBR.
8. Wheeler, O.E., "Spectrum Loading and Crack Growth", Tran. of the ASME - J. of Basic Engineering, Jan. 1972.
9. Elber, W., "The Significance of Crack Closure", in Damage Tolerance in Aircraft Structures, ASTM STP 486, 1971, p 230.
10. Gallagher, J.P., "Estimating Fatigue Crack Lives for Aircraft: Techniques", Experimental Mechanics, Vol. 16, Nov. 1976, pp 425-433.
11. Forman, R.G., Kearney, V.E., Engle, R.M., "Numerical Analysis of Crack Propagation in Cyclic - Loaded Structures", Trans. of the ASME - J. of Basic Engineering, Sept. 1967.
12. Schijve, J., "Fatigue Crack Growth Under Variable-Amplitude Loading", Eng. Fract. Mech., Vol. 11, 1979, pp 207-221.
13. Gallagher, J.P. and Stalnaker, H.D., "Developing Normalized Crack Growth Curves for Tracking Damage in Aircraft", J. of Aircraft Vol. 15, No. 2, Feb. 1978, pp 114-120.
14. Brussat, T.R., "Rapid Calculation of Fatigue Crack Growth by Integration", in Fracture Toughness and Slow - Stable Cracking, ASTM STP 559, 1974, pp 298-311.
15. Broek, D. and Smith, S.H., "The Prediction of Fatigue Crack Growth Under Flight-by-Flight Loading", Eng. Fract. Mech., Vol. 11, 1979, pp 123-141.
16. "Marker Band Evaluation, Analysis and Result", Fairchild Republic Co., Report No. FRC SA160R9416, 15 March 1979.
17. 1978 Annual Book ASTM Standard Part 10, pp 662-680.
18. Damage Tolerant Design Handbook, January 1975.
19. Parker, G.S., "Generalized Procedures for Tracking Crack Growth in Fighter Aircraft", AFFDL-TR-76-133, January 1977.
20. Tweed, J., Rooke, D.P., "The Elastic Problem for an Infinite Solid Containing a Circular Hole with a Pair of Radial Edge Cracks of Different Lengths", Int'l J. Eng'g. Science, 1976, Vol. 14, pp 925-933.
21. Isida, M., "Stress Intensity Factors for the Tension of an Eccentrically Cracked Strip", Trans. of the ASME - J. of Applied Mechanics, Sept. 1966, pp 674-675.
22. Brussat, T.R., Chiu, S.T., "Flaw Growth in Complex Structure", LR 28, Vol. I, 10 June 1977.
23. Levy, M., Kuo, A.S., Grube, K., "Practical Method of Fatigue Crack Growth Analysis for Damage Tolerance Assessment of Aluminum Structure in Fighter-Type Aircraft", AIAA 18th Aerospace Sciences Meeting, Jan. 14-16, 1980, Pasadena, California.